PROGRESS ON UPGRADES TO CCL RESONANCE CONTROL AT LANSCE

W. Hall†, M. Rodriguez, J. Valladares, J. Vega, Los Alamos National Laboratory, Los Alamos, United States

Abstract

The resonance control system for the cavity-coupled linear accelerator (CCL) portion of the Los Alamos Neutron Science Center (LANSCE) has been a consistent source of operational downtime. The present system has been used since installation with only minor upgrades, so a system is being developed to replace it with modern components to reduce maintenance and downtime. The present control algorithm maintains water temperature at a set point based on the average RF power, and other parameters that are direct indications of resonance such as the cavity field phase or its ratio to forward power should be implemented to improve issues inherent to the present control system. These relevant data have been collected for several RF modules and analyzed. Additionally, the control of the valve used to maintain water temperature is antiquated, and a commercially available off-the-shelf stepper motor driver is required as other parts are upgraded. A prototype of a new system is discussed.

INTRODUCTION

The Los Alamos Neutron Science Center (LANSCE) accelerates H^+ and H^- through a drift tube linear accelerator (DTL) to 100 MeV, and the H^- beam continues acceleration up to 800 Mev through 44 cavity coupled linear accelerator (CCL) modules. This facility has delivered beam at this energy since 1972, and many systems have undergone few changes in the subsequent decades. One such system in the resonance control used for the CCL.

The CCL operates at a frequency of 805 MHz with a peak power between 500 and 1200 kW, and with a pulse repetition rate of 120 Hz and a pulse width of about 1ms, there is about 50 to 140 kW average power that must be dissipated in the cooling system. The cooling system is also the method for maintaining resonance at 805 MHz and consists of a tank that mixes the water in the cooling loop with a variable amount of chilled water. The flow of chilled water that is input into the mix tank is varied by a stepper motor-controlled valve, and the electronic control is automated based upon average RF measurements. A schematic of the system is shown in Fig. 1.

The control method of the water temperature has several flaws that have resulted in beam downtime and extensive labor throughout the life of the CCL. The control system has four temperatures readings of the inlet and outlet going in two directions across the length of the CCL module, and the average of these readings is maintained at a temperature that is set by the measurement of average RF. The proper operation requires the temperature near zero average RF power and at high average RF power to be set individually by adjusting two potentiometers until the reflected power is minimized for each condition. The desired water temperature is then determined by a linear interpolation based on those two points.

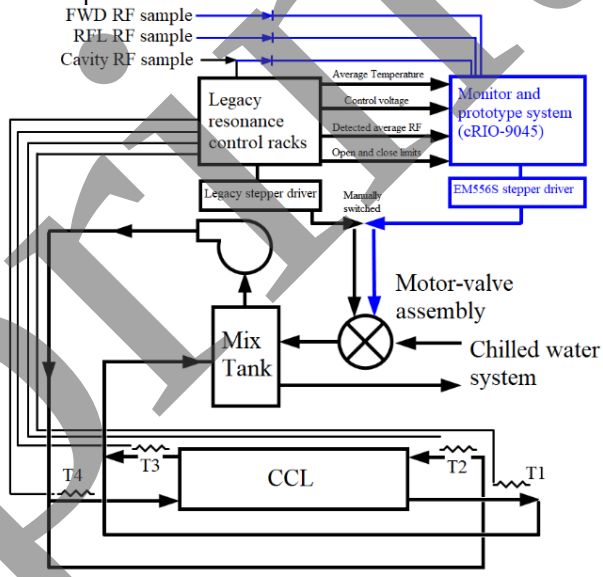

Figure 1: Block diagram of resonance control system. The present system is in black and the monitor and prototype system is in blue.

This process is performed each year, and some of the issues that have occurred in the past several years include: bad thermistor contacts, improper RF attenuation due to changes in tuning, and shifts in required temperature or poor initial settings. These issues necessitate an upgrade to the system.

A monitor and prototype system has been developed using a cRIO-9045 to both log key data and to demonstrate methods of control. The cRIO uses the FPGA module for signal collection, and the real-time application runs with UI output to a monitor. Several temperature control methods based on those signals were then developed to progressively build toward an autonomous system. The interaction of this system to the present resonance control is also shown in blue in Fig 1.

LEGACY SYSTEM MONITORING

The FPGA is used to read both pulsed RF signals and DC signals that are output from the original resonance control system. These signals have been used in the past to

†twh@lanl.gov

*Work was performed under the auspices of the US Department of Energy by Triad National Security, LLC, under contract 89233218CNA000001.

monitor and troubleshoot systems that are not operating correctly. A history of values is then stored in the real-time application for tracking trends while the system is being actively monitored, and these values can also be written to files for later analysis.

Data Collection

The FPGA runs on a 15µs loop to collect both the pulsed and DC data. The forward and reflected power and the cavity field are passed through a diode detector, and their envelopes are measured in a NI-9401 module. One of these or a fourth signal can be used as a trigger that collects the average value of each signal within a gate. This gate is typically a few hundred µs after the start of the pulse and a few dozen µs wide.

The DC signals are outputs of the present resonance control system. The four temperature probes are averaged in an analog circuit and output to the front panel, and this output voltage is 1V for every degree Fahrenheit above or below the nominal 0V at 80°F. An average power detector is also used, and a voltage is output to both the controller and the front panel. The temperature signal is compared to the set point based on the average RF power, and temperature is then controlled by an analog PD loop. The output of that loop is a voltage that goes to a voltage controlled oscillator that commands the in-house designed stepper driver. This PD loop voltage is also monitored.

Legacy System Performance

The data collected from several modules provided insights into how available signals can be used for resonance control. Data was collected with repetition rates of 10 Hz and 60 Hz, and the temperature during control with RF had a range of about 1.2°F at 10 Hz and about 0.3°F at 60 Hz. The higher repetition rate will heat the water, which makes changes to the chilled water flow into the mix tank more responsive, explaining the tighter control.

The legacy system performance was also compared to the calculated response of the control methods before attempting to implement them. The data points used for the steepest descent calculation described in the next section were collected along with the real-time data, and it is apparent that the data collected at the real-time rate (~0.2-2s) would be sufficient for calculating stepper motor speed. This would require fewer points to get a smoother response, so a timer was added to calculate the motor speed within the FPGA at this rate.

The data collected by the Real-Time application at 1 s intervals was then used to determine what control signal would be calculated. The summations used in calculations add six blocks of variable numbers of data points, so the sample size is one variable that can be adjusted so that the control signal is smooth and does not have substantial sign reversals to ensure good motor control. Using 30-60 samples for this calculation do this adequately, but 120 or more samples show significant improvement. Figure 2 shows the return loss versus temperature for module 11. The temperature was delayed by 40 s in this figure and compared to the as-is data. The tighter correlation between temperature and return loss is indicative of the delay between the peaks in the oscillations of temperature and return loss. This might indicate that a delay on the temperature is needed for control, but the control calculations also have a natural delay that might be sufficient. This data also shows the behavior that was expected with return loss minimized at some temperature (81.15°F) and increasing away from it. It should also be noted that the indexing of the power measurements was too far into the RF pulse, so different sets of return loss were captured depending on beam status.

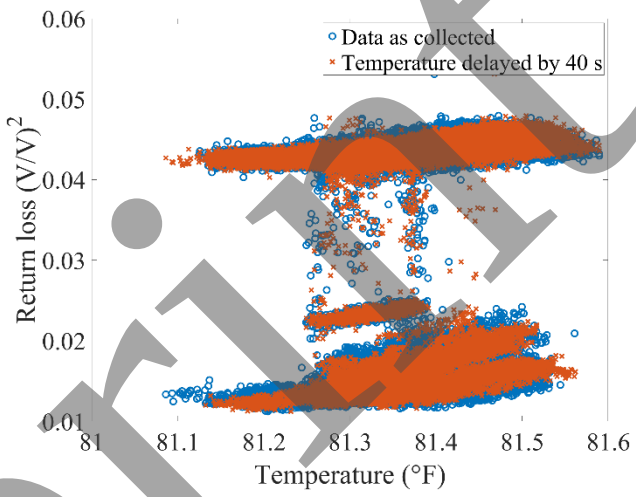

Figure 2: Data collected for module 11 with RF at 60 Hz.

PROTOTYPING AND CONTROL METHODS

The addition of control methods was achieved relatively easily and allowed for prototyping. Two stepper motor drivers were tested to allow for control of the valve with modern equipment that can be controlled by digital cRIO outputs. The output of the cRIO is controlled by one of several methods.

A manual output was first used to test the chain from the cRIO to the stepper driver and ultimately the stepper motor valve assembly. This was first tested on the bench then at several modules. Two commercial stepper drivers were tested, and both were able to control the motor on the benchtop. Only the Leadshine EM556S was used for the rest of the testing because of its simplicity in implementation. The manual control of the motors installed in several modules was also tested, and the open-to-close time was found to be about 26-28 s 4 microsteps at a rate of 500 Hz. This speed is consistent with the present system. The prototype also works well with 2 microsteps at half the speed.

The next step was to see if the cRIO could maintain a fixed temperature. The temperature should remain at a constant level when there is no RF, and with RF relatively constant, there should also be little variation in temperature, so maintaining a thermostatic condition was also important. A PID control loop was used for this, with samples taken at defined time intervals of about 0.5 s to be consistent with findings of the previous section. The derivative portion of the control loop is calculated with a linear least squares fit of the temperature to sample number. This requires

summations of the sample number n_i and the temperature T_n over N samples to get

$$\frac{dT}{dn} = \frac{N\sum_{n=0}^{N-1} nT_n - \sum_{n=0}^{N-1} n \sum_{n=0}^{N-1} T_n}{N\sum_{n=0}^{N-1} n^2 - \left(\sum_{n=0}^{N-1} n\right)^2} \quad (1)$$

This method was implemented with some success, but there was substantial noise on the temperature signal that affected the motor speed via the proportional component. The sample number was increased from 8 to 18 and the average was used for the proportional signal to mitigate this. The calculated control speeds are shown in Fig. 3, and these adjustments did improve the noise of the system substantially.

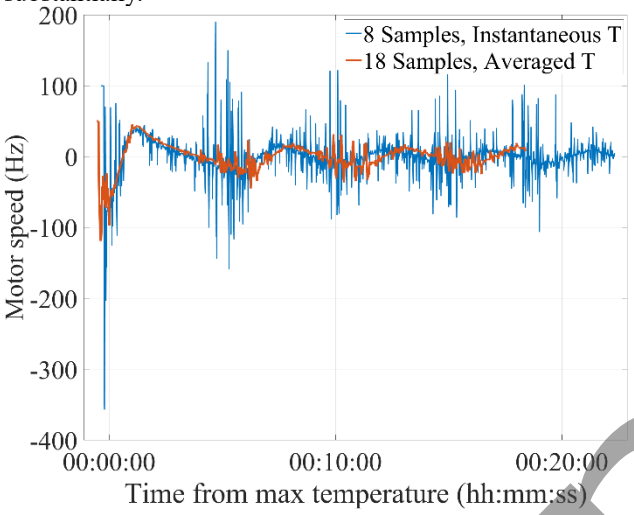

Figure 3: Calculated step rate for two methods using K_p=50 and K_d=1000 and controlling to 85°F.

The gains of the temperature control were adjusted to maintain temperature to a similar range as the legacy system. Several gains used to control the system to 86°F are shown in Fig. 4. The proportional and derivative gains (K_p and K_d respectively) of 100 and 4000 maintained a temperature range of about 85.95 to 86.15°F, which is similar to the range of control with RF. The integral gain was always set to zero and is not present in the legacy system. In addition to these methods, the control signal of the legacy system was multiplied by 50, and this maintained good control of temperature without RF. This could be an important setting to quickly regain control while testing control methods with RF.

The last method is to implement temperature control based on the RF signals. The present resonance control system is based on secondary effects, but the upgrade should allow for direct control based on RF. The prototype system has a PID loop that can control on phase between the forward power and reflected or cavity field signals, but this does require the phase to be set up well. A simple mixer could be used for the phase detection, or a 360° phase detector like that proposed by Potter [1] could be integrated into the controller.

Another method is to minimize the reflected to forward power ratio (return loss) or to maximize the cavity field to forward power. A steepest descent method to minimize reflected power for resonance control has been investigated by others previously [2, 3], and a simple linear least squares fit of the return loss to temperature has been programmed in the prototype. This allows the derivative of the return loss to be found using N sets of data in an expression analogous to Eq. 1. The use of estimated motor position in place of the temperature is also proposed for investigation. This would eliminate the need for thermistors, which have been temperamental, but it is not clear if this method will be viable.

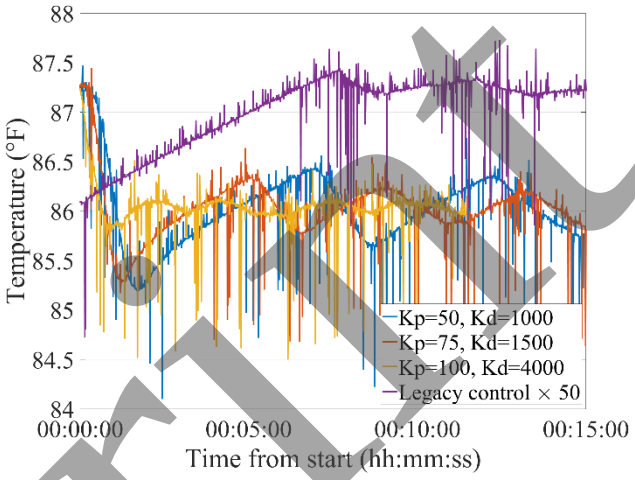

Figure 4: Temperature during control with PID loop and several combinations of gains and with the legacy control voltage controlling the output of the prototype system.

FUTURE WORK

The work done so far in documenting resonance control performance and prototyping control methods has been promising, and there are many improvements that can be implemented as a permanent system is developed. First, the noise of the stepper driver should be addressed. A new driver could be changed in conjunction with the motor-valve assembly to add a radiation-hardened position measurement and a more linear valve.

The control with RF will be tested. In addition to adjustments for control at start-up and nearly constant RF levels, water temperature should control to a certain temperature at turn off. Ideally, the control method should be able to adjust to this point without being manually set. Additionally, more sophisticated control methods might be investigated by the machine learning team at LANSCE.

Once the hardware and control methods are decided upon, a final architecture can be designed. This would have separate analog to digital converters to measure the necessary signals, and a microcontroller or FPGA could be built into a chassis for installation.

REFERENCES

[1] J. M. Potter, "Novel RF Phase Detector for Accelerator Applications", in *Proc. NAPAC'22*, Albuquerque, NM, USA, Aug. 2022, pp. 446-448. doi:10.18429/JACoW-NAPAC2022-TUPA43

[2] A. Scheinker, "Application of Extremum Seeking for Time-Varying Systems to Resonance Control of RF Cavities," *IEEE Trans. Control Syst. Technol.*, vol. 25, no. 4, pp. 1521–1528, Jul. 2017. doi:10.1109/tcst.2016.2604742

[3] R. Leewe, “RF cavity tuning based on reflected power measurements”, Ph.D. thesis, School Mechatronic Syst. Eng., Simon Fraser University, 2017.